

Observation of the Second Harmonic in the Phase Dependence of a Superconducting Current in Nb/Au/YBCO Heterojunctions

P. V. Komissinskiĭ^{1,2}, G. A. Ovsyannikov¹, E. Il'ichev³, and Z. Ivanov²

¹ Institute of Radio Engineering and Electronics, Russian Academy of Sciences, Moscow, 103907 Russia
e-mail: gena@hitech.cplire.ru

² Chalmers University of Technology, S 411 96 Göteborg, Sweden

³ Institute for Physical High Technology, Department of Cryoelectronics, P.O. Box 100239, D-07702 Jena, Germany

Received February 21, 2001; in final form, March 12, 2001

The second harmonic in the dependence of a superconducting current on the phase difference of superconducting wave functions of the electrodes was observed experimentally in Nb/Au/(001)YBa₂Cu₃O_x heterojunctions. Possible reasons for its appearance were discussed within the framework of a mixed ($d \pm s$) symmetry order parameter of YBa₂Cu₃O_x. © 2001 MAIK "Nauka/Interperiodica".

PACS numbers: 74.80.Dm; 73.40.-c

It is presently known that the majority of metal oxide high- T_c superconductors (MOHTS) are characterized by the d symmetry of the superconducting order parameter [1]. This was most clearly manifested in experiments on studying superconducting quantum interference devices (SQUIDs) containing junctions of a conventional (with the s -type symmetry of the order parameter) superconductor (S) connected to two orthogonal directions of the MOHTS basal plane [2]. The problem of electron transport in MOHTS/S junctions (here, the slash designates a potential barrier) in the direction perpendicular to the MOHTS basal plane still remains unclear [3–6]. Because of the d symmetry of the order parameter in MOHTSs, the superconducting current in these heterojunctions must be small (proportional to the second degree of the averaged interface transmittance \bar{D}^2) and must vary with the phase difference two times more frequently. That is, the superconducting current must contain a component corresponding to the second harmonic of the current–phase relation (CPR) [7]. However, the critical current observed in the experiments [3–6] multiplied by the normal resistance depends only slightly on the interface transmittance; however, it decreases if an epitaxial MOHTS film is used instead of a single crystal [5]. The experimental data can be explained based on the assumption that the MOHTS is characterized by the mixed s – d symmetry of the superconducting order parameter, with the s -wave component changing its sign (that is, changing its phase by π) and the d -wave component remaining unchanged at the twin boundary [6]. Studying the appearance of microwave-induced Shapiro steps in CPRs of Pb/YBa₂Cu₃O_x junctions demon-

strated that the second harmonic is absent in the CPR with an accuracy of up to 5% [5].

In this work, we report an experimental study of CPRs for heterojunctions constructed of niobium (s -wave superconductor) and a c -oriented YBa₂Cu₃O_x (YBCO) film with an additional gold interlayer (Nb/Au/YBCO). The CPRs were measured using a radiofrequency superconducting quantum interference device (SQUID). The second harmonic of the CPR was found in the experiment. Estimates were given indicating that electron transport in heterojunctions on (001) YBCO is determined by the contact between the s -wave and (d – s)-wave superconductors.

Epitaxial (001) YBCO films 150 nm thick were grown by laser deposition on (001) LaAlO₃ and (001) SrTiO₃ substrates. The superconducting transition temperature of films was measured by the magnetic induction method and was found to be $T_c = 88$ – 90 K. Immediately after deposition, the YBCO film was coated with a thin Au layer without breaking a vacuum, which prevented the YBCO surface from degradation. This allowed interfaces to be obtained with a low characteristic resistance $r \equiv R_N A = 10^{-5}$ – 10^{-6} Ω cm² (R_N and A are the normal resistance and the contact area, respectively). The Nb film was deposited by dc magnetron sputtering. Note that the direct Nb/YBCO contact gave the boundary with a considerably higher characteristic resistance $r \sim 10^{-2}$ Ω cm². Photolithography and ion-beam etching with low-energy argon ions were used to form the geometry of Nb/Au/YBCO heterojunctions (the thickness of gold is 8–20 nm, and niobium, 200 nm). The current in these heterojunctions flows perpendicular to the substrate (along the c axis of

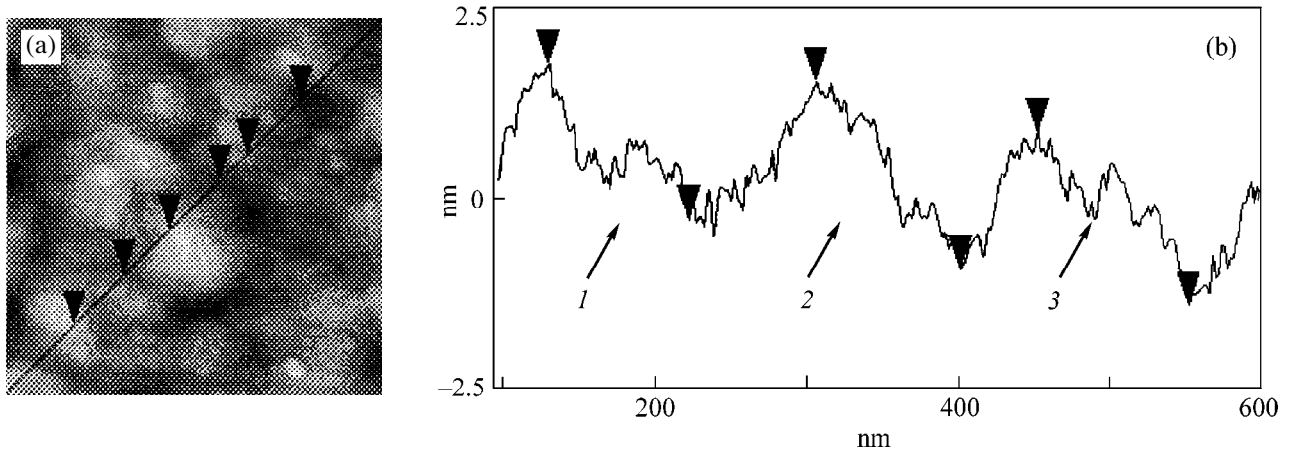


Fig. 1. (a) Two-dimensional profile of a (001) YBCO film obtained using an atomic force microscope; (b) film cross section. Numbers indicate film areas in which distances between the marks were measured. The largest horizontal and vertical distances between the marks are 100 and ~ 3 nm, respectively; that is, $\gamma \approx 2^\circ$.

YBCO), and there is no contact with the basal plane of the YBCO film [8, 9].

To reduce the effect of transport along the basal plane due to the roughness of the surface, the growth process was optimized with the aim to obtain YBCO films with a smooth surface. The morphology of films was monitored in test samples using a high-resolution atomic force microscope. The greatest surface roughness of the (001) YBCO films used in heterojunctions (calculated as the difference between the points of the maximum and minimum deviations from the substrate plane) was 3 nm, with the horizontal distance between these points equal to 100 nm (Fig. 1). Hence, the typical average angle of inclination of YBCO-film surface areas to the (001) YBCO plane can be estimated at $\gamma \approx 2^\circ$. The contribution to the measured resistance of electron transport due to contact with the basal plane of the YBCO film was estimated by calculating the characteristic resistance r of the boundaries between Au and YBCO [8, 9]. The resistance r of heterojunctions was determined from the condition that the resistances of the boundaries between Au and YBCO along the c axis (r_c) and in the basal plane of YBCO (r_{ab}) are connected in parallel. These resistances are due to the mismatch between the Fermi velocities of the contacting materials with a sharp interface:

$$r = r_c r_{ab} / (r_{ab} + r_c \tan \gamma), \quad (1)$$

where $\tan \gamma \approx A_{ab}/A$, and A_{ab} is the total area of contacts with the basal plane of the YBCO film. The inclined film surfaces were replaced by a set of (001) YBCO planes and planes perpendicular to them with characteristic resistances r_c and r_{ab} , respectively. It was shown in [9] for the typical Fermi-momentum anisotropy of order 3 that r_c exceeds r_{ab} by no more than an order of magnitude. Hence, the current through the contact with the basal plane is small for the surface roughness observed experimentally ($\gamma \approx 2^\circ$). This is confirmed by

the absence of the conductance peak in Nb/Au/YBCO junctions at temperatures above the critical temperature of niobium and small biases [the anomaly caused by the Andreev reflection in a d -wave superconductor (D)]. Theory predicts the appearance of the given anomaly for a rough boundary of N/D heterojunctions (N is a normal metal) even in the case of an arbitrarily oriented d -wave superconductor [10]. Note that the current through superconducting short circuits formed by pinholes in the Au film between Nb and YBCO is small, because r measured for the Nb/YBCO boundary exceeds the resistance of the Au/YBCO boundary by 3–4 orders of magnitude [8].

Electrophysical properties were measured for more than 20 single junctions of sizes from 10×10 to $100 \times 100 \mu\text{m}$ and five radiofrequency SQUIDs. The table presents typical parameters of single junctions for which the critical current grows with an increase in area. For the junctions studied, the critical current density was in the range $j_c = 1\text{--}12 \text{ A/cm}^2$, whereas $I_c R_N = 10\text{--}90 \mu\text{V}$, where R_N is the normal junction resistance determined from the differential junction resistance R_d at bias $V \approx 2 \text{ mV}$. The current–voltage characteristic (I – V curve) and the voltage dependence of the differential junction resistance R_d are shown in Fig. 2. At small biases, the junction I – V curve closely corresponds to the resistive model of a small-capacitance Josephson junction. With increasing bias $V > 2 \text{ mV}$, the I – V curve takes the form $V = (I + I_e)R_N$, where $I_e < 0$. The excess current $I_e > 0$ is observed in all superconducting junctions with direct (nontunnel-type) conductivity [11]. Negative I_e (low current) is a characteristic feature of superconducting two-barrier S/N/S' heterostructures, in which I_e changes its sign (transition from excess to low current takes place) as the neighborhood effect in the N interlayer decreases [12–14]. It is seen in Fig. 2 that the

junction I - V curves at high biases are described well by the equation [12]

$$V = IR_N + I_e R_N \tanh(eV/kT), \quad (2)$$

which is typical for S/N/S' structures. For the junction shown in Fig. 2, $I_e = -145 \mu\text{A}$ at $T = 4.2 \text{ K}$. According to the calculation [14], the experimental parameters of the structures studied must give $I_e = (-\bar{D}_1 \Delta_{\text{YBCO}} - \Delta_{\text{Nb}})/(eR_N) \approx -270 \mu\text{A}$, where $r = 10^{-5}$ - $10^{-6} \Omega \text{ cm}^2$ determines the direction-averaged transmittance of the Au/YBCO interface $\bar{D}_1 = 2\rho_c l/3r = 10^{-4}$ - 10^{-5} , Δ_{YBCO} is the YBCO order parameter, $\Delta_{\text{Nb}} = 1.2 \text{ mV}$ is the Nb gap, and $\rho_c \approx 10^{-2} \Omega \text{ cm}$ and $l \approx 1 \text{ nm}$ are, respectively, the resistivity of and the mean free path in the YBCO film in the c direction [9].

A singularity is observed in the $R_d(V)$ curve as a decrease in R_d at $V = 1.2 \text{ mV}$, which corresponds to Δ_{Nb} in magnitude. Its temperature dependence is close to that predicted by the BCS theory. The singularity in the I - V curve disappears together with the critical current at $T = 8.5$ - 9.1 K . The temperature dependence $I_c(T)$ is close to $\Delta_{\text{Nb}}(T)$. Note that gap singularities in an s -wave superconductor (Pb) were observed previously in Pb/YBCO [5, 6].

In order to measure the CPR, a SQUID was formed from a junction $10 \times 10 \mu\text{m}$ in size short-circuited by a YBCO film with an inductance $L \approx 80 \text{ pH}$ and by a junction of a considerably larger area of $100 \times 100 \mu\text{m}$. The SQUID impedance was measured as a function of the external magnetic flux Φ_e with the use of an oscillatory circuit inductively coupled to a ring. The phase difference φ across the junction under study is determined by the magnetic flux in the ring Φ_i as follows: $\varphi = 2\pi\Phi_i/\Phi_0$, where $\Phi_0 = h/2e = 2.07 \times 10^{-15} \text{ T m}^2$ is

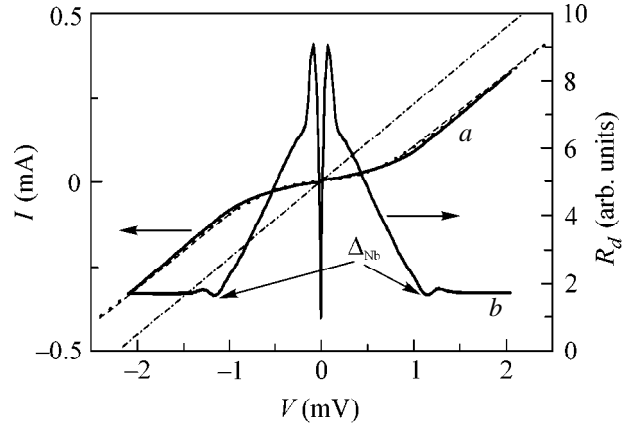


Fig. 2. a I - V curve and b voltage dependence of the differential resistance of a heterostructure at $T = 4.2 \text{ K}$. The dependence obtained from Eq. (2) is shown in the I - V curve by the dashed line; Ohm's law $V = IR_N$ is shown by the dot-and-dash line.

the magnetic flux quantum. The CPR $f(\varphi) = I_s(\varphi)/I_c$ is determined from measurements of the phase difference α between the driving high-frequency current and the voltage across the circuit

$$\tan \alpha = k^2 Q i_c f'(\varphi)/(1 + i_c f'(\varphi)), \quad (3)$$

where $f'(\varphi) = df(\varphi)/d\varphi$, $\varphi_e = 2\pi\Phi_e/\Phi_0$ is the normalized external magnetic flux, $i_c = 2\pi LI_c/\Phi_0$ is the normalized critical current of the junction, and Q is the quality factor of the oscillatory circuit. The CPR is calculated from experimental data by Eq. (3) at $i_c < 1$. In this case, we neglect the effect of junction capacitance [15].

Experimental $I_s(\varphi)$ curves are shown in Fig. 3 for several temperatures. As the temperature decreases, the

Parameters of the Nb/Au/YBCO heterojunctions measured at $T = 4.2 \text{ K}$

Junction no.	$A, \mu\text{m}^2$	d, nm	$I_c, \mu\text{A}$	$J_c, \text{A/cm}^2$	R_N, Ω	$R_N A, \mu\Omega \text{ cm}^2$	$I_c R_N, \mu\text{V}$	$\Delta_{\text{Nb}}, \text{mV}$
SQ1J1	100	20	5	5	4.4	4.4	22	1.2
SQ1J3	10000	20	181	1.81	0.15	15	27	-
SQ1J5	100	20	1.5	1.5	18.3	18.3	27.5	0.8
SQ3J1	100	20	1	1	68	68	68	1.1
SQ7J10	225	8	15	6.7	5.1	11.5	76.5	1.1
SQ7J11	10000	8	234	2.3	0.05	5	11.7	-
SQ7J3	625	8	20	3.2	1.3	8.1	26	1.1
SQ7J4	900	8	23	2.6	0.83	7.5	19.1	1.2
SQ7J13	400	8	10	2.5	1	4	10	-
SQ7J15	400	8	16	4	1.8	7.2	28.8	-
SQ7J17	100	8	2	2	18.8	18.8	37.6	1.2
SQ7J18	100	8	3	3	10	10	30	-
SQ10J3	100	18	1.2	1.2	60	60	72	1.2

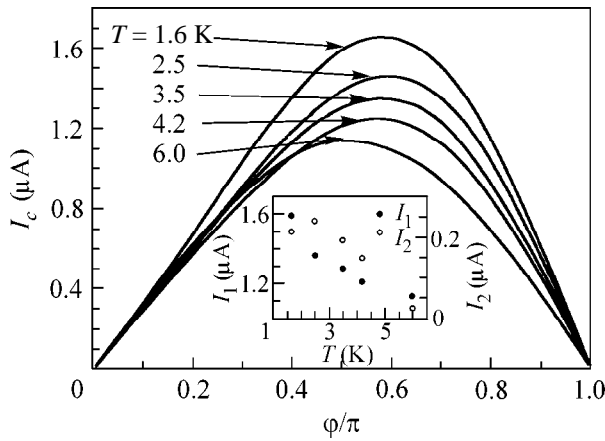


Fig. 3. Transformation of the CPR of a heterostructure as a function of temperature. The inset shows the temperature dependence of the first and the second harmonics of the Fourier transform of CPR.

CPR exhibits a transformation that corresponds to the appearance of the second harmonic of its Fourier expansion in terms of ϕ . Taking into account only two harmonics, one obtains $I_s(\phi) = I_1 \sin \phi + I_2 \sin(2\phi + \phi)$. If, following [5], the occurrence of two harmonics of the CPR is explained by the combined d - and s -wave symmetry of the YBCO order parameter, then an agreement with the experiment is observed for d - s ($\phi = \pi$). Using the theoretical approach [7], according to which the YBCO order parameter can be represented as $\Delta_{\text{YBCO}}(\theta, \psi) = \Delta_{d\text{-YBCO}} \sin^2 \theta \cos(2\psi) - \Delta_{s\text{-YBCO}}$ (θ and ψ are the azimuthal and radial angles, respectively), and assuming that $\Delta_{\text{Nb}}(\theta, \psi) = 1.2$ mV for niobium, we find that the theory [7] gives the best agreement with the experiment at $T = 1.7$ K for the following parameters: $\Delta_{d\text{-YBCO}} = 20$ mV, $\Delta_{s\text{-YBCO}} = 0.45$ mV, and the averaged barrier transmittance $\bar{D} \approx 3 \times 10^{-2}$.¹

At the same time, the amplitudes of higher harmonics of the expansion of $I_s(\phi)$ in terms of $\sin(n\phi)$ for a tunnel junction with interface transmittance \bar{D}_1 are proportional to the higher degrees of interface transmittance and to the gap ratio; that is, $I_2/I_1 \approx \bar{D}_1 \Delta_{\text{Nb}}/\Delta_{s\text{-YBCO}} \sim \bar{D}_1$. Hence, within the framework of this simple estimate, $I_2/I_1 \sim 10^{-4}$ – 10^{-5} . However, the experiment at $T = 1.7$ K gives $I_2/I_1 \sim 0.16$. It may well be that the following two factors are determining, although not taken into account in these simple estimates.

The first factor is the twinning of the (001) YBCO film, which leads to the sign reversal of the s -wave component at the twin boundary and, hence, decreases the amplitude I_1 because of the mutual compensation of contributions from the domains with different signs of

s -wave component. In the case of equal areas of the twin domains, I_1 must equal zero, and I_2 must increase proportional to \sqrt{N} in the case of a random scatter of twin-boundary sizes, where N is the number of twin boundaries in the heterojunction [6, 16]. The dependence of the critical current on the junction area in our experiment is not proportional to \sqrt{N} (see table), though this proportionality is typical for the random distribution of twin domain sizes. In fact, a critical current from an uncompensated part δ of domains is observed. The total superconducting current from the s -wave component in a heterojunction of the same area on an untwinned (001) YBCO film must be higher by a factor of δ^{-1} . In this case, the model of a Josephson junction with an alternating current density [17] applies qualitatively to the heterojunction under study. This model predicts that the amplitude of the second harmonic in the current–phase relation is significant [18]. However, further investigations are required for a quantitative comparison to be made between the theory and experiment.

Note that the contribution of the d -wave component is independent of the number and the size distribution of twin boundaries and that we do not observe the ($d + is$)-wave component (i is the imaginary unit). This component may arise either because of the influence of twin-boundary vicinity, where the sign changes from $d + s$ to $d - s$ [16], or due to the sign reversal of the s -wave component near the YBCO film surface [19].

The second possible reason for the existence of anomalously high I_2 is the fact that a Nb/Au interface with transmittance $\bar{D}_2 \approx 10^{-1}$ occurs in Nb/Au/YBCO. It is evident in Fig. 2 that this interface affects the I - V curve. Actually, the second harmonic of the CPR may appear in the case of a strongly asymmetric two-barrier structure [20]. On the other hand, simple estimates following from Eq. (9) of [20] indicate that $I_2/I_1 \propto \bar{D}_1$ for the Nb/Au/YBCO heterostructures studied in this work, and, hence, the second harmonic amplitude of the CPR is small. However, the ultimate answer to the question of the Nb/Au interface effect on the CPR in Nb/Au/YBCO heterostructures can be determined only after accurate numerical calculations.

Note in conclusion that, although general regularities were found in the behavior of the heterojunctions studied (I - V curve shape, temperature dependence of the critical current, gap singularity due to niobium, etc.), a rather large scatter (up to 100%) was observed for quantitative parameters such as interface resistance, critical current density, and ratio of the first and the second harmonics of the CPR. Here, along with the Au/YBCO interface, the Nb/Au interface and the twinning of YBCO films are key factors that are difficult to control by electrophysical methods.

We are grateful to D.V. Balashov, P.N. Dmitriev, S.A. Kovtonyuk, and K.I. Konstantinyan for assistance

¹ $\Delta_{\text{YBCO}}(\theta, \psi)$ is normalized as $(1/2\pi) \int_0^{2\pi} \int_0^{\pi/2} \Delta_{\text{YBCO}}(\theta, \psi) \sin \theta d\theta d\psi = \Delta_{d\text{-YBCO}}$ [7].

in measurements and to A.V. Zaitsev, T. Klaeson, M.Yu. Kupriyanov, T. Lofwander, P.B. Mozhaev, I. Tanaka, A. Tsalenchuk, and V. Shumeiko for useful discussions.

This work was supported in part by the Russian Foundation for Basic Research, the federal program "Topical Problems of Condensed Matter Physics," the subprogram "Superconductivity," the European INTAS program, the Sweden consortium for studying new materials, and the "Science for Peace" program (project no. 973559).

REFERENCES

1. C. C. Tsuei and J. R. Kirtley, *Rev. Mod. Phys.* **72**, 969 (2000).
2. D. A. Wollman, D. J. van Harlingen, W. C. Lee, *et al.*, *Phys. Rev. Lett.* **71**, 2134 (1993).
3. H. Akoh, C. Camerlingo, and S. Takada, *Appl. Phys. Lett.* **56**, 1487 (1990).
4. A. G. Sun, D. A. Gajewski, M. B. Maple, *et al.*, *Phys. Rev. Lett.* **72**, 2267 (1994).
5. R. Kleiner, A. S. Katz, A. G. Sun, *et al.*, *Phys. Rev. Lett.* **76**, 2161 (1996).
6. K. A. Kouznetsov, A. G. Sun, B. Chen, *et al.*, *Phys. Rev. Lett.* **79**, 3050 (1997).
7. Y. Tanaka, *Phys. Rev. Lett.* **72**, 3871 (1994).
8. P. V. Komissinskiĭ, G. A. Ovsyannikov, N. A. Tulina, *et al.*, *Zh. Éksp. Teor. Fiz.* **116**, 2140 (1999) [*JETP* **89**, 1160 (1999)].
9. P. V. Komissinskiĭ, G. A. Ovsyannikov, and Z. G. Ivanov, *Fiz. Tverd. Tela (St. Petersburg)* **43**, 769 (2001) [*Phys. Solid State* **43**, 801 (2001)].
10. M. Fogelström, D. Rainer, and J. A. Sauls, *Phys. Rev. Lett.* **79**, 281 (1997).
11. K. K. Likharev, *Rev. Mod. Phys.* **51**, 101 (1979).
12. A. V. Zaitsev, *Pis'ma Zh. Éksp. Teor. Fiz.* **51**, 35 (1990) [*JETP Lett.* **51**, 41 (1990)].
13. G. E. Babayn, L. V. Filippenko, G. A. Ovsyannikov, *et al.*, *Supercond. Sci. Technol.* **4**, 476 (1991).
14. A. F. Volkov, A. V. Zaitsev, and T. M. Klapwijk, *Physica C (Amsterdam)* **210**, 21 (1993).
15. E. Il'ichev, V. Zakosarenko, V. Schultze, *et al.*, *Appl. Phys. Lett.* **72**, 731 (1998); E. Il'ichev, V. Zakosarenko, R. P. J. Ijsselsteijn, *et al.*, *Phys. Rev. Lett.* **81**, 894 (1998).
16. M. Sigrist, K. Kuboki, P. A. Lee, *et al.*, *Phys. Rev. B* **53**, 2835 (1996).
17. R. G. Mints, *Phys. Rev. B* **57**, R3221 (1998).
18. E. Il'ichev, V. Zakosarenko, R. P. J. Ijsselsteijn, *et al.*, *Phys. Rev. B* **59**, 11 502 (1999).
19. R. Haslinger and R. Joynt, *J. Phys.: Condens. Matter* **12**, 8179 (2000).
20. M. Yu. Kupriyanov, A. Brinkman, A. A. Golubov, *et al.*, *Physica C (Amsterdam)* **326–327**, 16 (1999).

Translated by A. Bagatur'yants